Coherent ρ^0 Production in Ultraperipheral Heavy-Ion Collisions

C. Adler,[11] Z. Ahammed,[23] C. Allgower,[12] J. Amonett,[14] B. D. Anderson,[14] M. Anderson,[5] G. S. Averichev,[9] J. Balewski,[12] O. Barannikova,[9,23] L. S. Barnby,[14] J. Baudot,[13] S. Bekele,[20] V.V. Belaga,[9] R. Bellwied,[31] J. Berger,[11] H. Bichsel,[30] L. C. Bland,[2] C. O. Blyth,[3] B. E. Bonner,[24] A. Boucham,[26] A. Brandin,[18] A. Bravar,[2] R.V. Cadman,[1] H. Caines,[20] M. Calderón de la Barca Sánchez,[2] A. Cardenas,[23] J. Carroll,[15] J. Castillo,[26] M. Castro,[31] D. Cebra,[5] P. Chaloupka,[20] S. Chattopadhyay,[31] Y. Chen,[6] S. P. Chernenko,[9] M. Cherney,[8] A. Chikanian,[33] B. Choi,[28] W. Christie,[2] J. P. Coffin,[13] T. M. Cormier,[31] J. G. Cramer,[30] H. J. Crawford,[4] W. S. Deng,[2] A. A. Derevschikov,[22] L. Didenko,[2] T. Dietel,[11] J. E. Draper,[5] V. B. Dunin,[9] J. C. Dunlop,[33] V. Eckardt,[16] L. G. Efimov,[9] V. Emelianov,[18] J. Engelage,[4] G. Eppley,[24] B. Erazmus,[26] P. Fachini,[2] V. Faine,[2] K. Filimonov,[15] E. Finch,[33] Y. Fisyak,[2] D. Flierl,[11] K. J. Foley,[2] J. Fu,[15,32] C. A. Gagliardi,[27] N. Gagunashvili,[9] J. Gans,[33] L. Gaudichet,[26] M. Germain,[13] F. Geurts,[24] V. Ghazikhanian,[6] O. Grachov,[31] V. Grigoriev,[18] M. Guedon,[13] E. Gushin,[18] T. J. Hallman,[2] D. Hardtke,[15] J.W. Harris,[33] T.W. Henry,[27] S. Heppelmann,[21] T. Herston,[23] B. Hippolyte,[13] A. Hirsch,[23] E. Hjort,[15] G.W. Hoffmann,[28] M. Horsley,[33] H. Z. Huang,[6] T. J. Humanic,[20] G. Igo,[6] A. Ishihara,[28] Yu. I. Ivanshin,[10] P. Jacobs,[15] W.W. Jacobs,[12] M. Janik,[29] I. Johnson,[15] P. G. Jones,[3] E. G. Judd,[4] M. Kaneta,[15] M. Kaplan,[7] D. Keane,[14] J. Kiryluk,[6] A. Kisiel,[29] J. Klay,[15] S. R. Klein,[15] A. Klyachko,[12] A. S. Konstantinov,[22] M. Kopytine,[14] L. Kotchenda,[18] A. D. Kovalenko,[9] M. Kramer,[19] P. Kravtsov,[18] K. Krueger,[1] C. Kuhn,[13] A. I. Kulikov,[9] G. J. Kunde,[33] C. L. Kunz,[7] R. Kh. Kutuev,[10] A. A. Kuznetsov,[9] L. Lakehal-Ayat,[26] M. A. C. Lamont,[3] J. M. Landgraf,[2] S. Lange,[11] C. P. Lansdell,[28] B. Lasiuk,[33] F. Laue,[2] A. Lebedev,[21] R. Lednický,[9] V. M. Leontiev,[22] M. J. LeVine,[2] Q. Li,[31] S. J. Lindenbaum,[19] M. A. Lisa,[20] F. Liu,[32] L. Liu,[32] Z. Liu,[32] Q. J. Liu,[30] T. Ljubicic,[2] W. J. Llope,[24] G. LoCurto,[16] H. Long,[6] R. S. Longacre,[2] M. Lopez-Noriega,[20] W. A. Love,[2] T. Ludlam,[2] D. Lynn,[2] J. Ma,[6] R. Majka,[33] S. Margetis,[14] C. Markert,[33] L. Martin,[26] J. Marx,[15] H. S. Matis,[15] Yu. A. Matulenko,[22] T. S. McShane,[8] F. Meissner,[15] Yu. Melnick,[22] A. Meschanin,[22] M. Messer,[2] M. L. Miller,[33] Z. Milosevich,[7] N. G. Minaev,[22] J. Mitchell,[24] V. A. Moiseenko,[10] C. F. Moore,[28] V. Morozov,[15] M. M. de Moura,[31] M. G. Munhoz,[25] J. M. Nelson,[3] P. Nevski,[2] V. A. Nikitin,[10] L.V. Nogach,[22] B. Norman,[14] S. B. Nurushev,[22] J. Nystrand,[15] G. Odyniec,[15] A. Ogawa,[21] V. Okorokov,[18] M. Oldenburg,[16] D. Olson,[15] G. Paic,[20] S. U. Pandey,[31] Y. Panebratsev,[9] S.Y. Panitkin,[2] A. I. Pavlinov,[31] T. Pawlak,[29] V. Perevoztchikov,[2] W. Peryt,[29] V. A. Petrov,[10] M. Planinic,[12] J. Pluta,[29] N. Porile,[23] J. Porter,[2] A. M. Poskanzer,[15] E. Potrebenikova,[9] D. Prindle,[30] C. Pruneau,[31] J. Putschke,[16] G. Rai,[15] G. Rakness,[12] O. Ravel,[26] R. L. Ray,[28] S.V. Razin,[9,12] D. Reichhold,[8] J. G. Reid,[30] F. Retiere,[15] A. Ridiger,[18] H. G. Ritter,[15] J. B. Roberts,[24] O.V. Rogachevski,[9] J. L. Romero,[5] C. Roy,[26] V. Rykov,[31] I. Sakrejda,[15] S. Salur,[33] J. Sandweiss,[33] A. C. Saulys,[2] I. Savin,[10] J. Schambach,[28] R. P. Scharenberg,[23] N. Schmitz,[16] L. S. Schroeder,[15] A. Schüttauf,[16] K. Schweda,[15] J. Seger,[8] D. Seliverstov,[18] P. Seyboth,[16] E. Shahaliev,[9] K. E. Shestermanov,[22] S. S. Shimanskii,[9] V. S. Shvetcov,[10] G. Skoro,[9] N. Smirnov,[33] R. Snellings,[15] P. Sorensen,[6] J. Sowinski,[12] H. M. Spinka,[1] B. Srivastava,[23] E. J. Stephenson,[12] R. Stock,[11] A. Stolpovsky,[31] M. Strikhanov,[18] B. Stringfellow,[23] C. Struck,[11] A. A. P. Suaide,[31] E. Sugarbaker,[20] C. Suire,[2] M. Šumbera,[20] B. Surrow,[2] T. J. M. Symons,[15] A. Szanto de Toledo,[25] P. Szarwas,[29] A. Tai,[6] J. Takahashi,[25] A. H. Tang,[14] J. H. Thomas,[15] M. Thompson,[3] V. Tikhomirov,[18] M. Tokarev,[9] M. B. Tonjes,[17] T. A. Trainor,[30] S. Trentalange,[6] R. E. Tribble,[27] V. Trofimov,[18] O. Tsai,[6] T. Ullrich,[2] D. G. Underwood,[1] G. Van Buren,[2] A. M. VanderMolen,[17] I. M. Vasilevski,[10] A. N. Vasiliev,[22] S. E. Vigdor,[12] S. A. Voloshin,[31] F. Wang,[23] H. Ward,[28] J.W. Watson,[14] R. Wells,[20] G. D. Westfall,[17] C. Whitten,, Jr.,[6] H. Wieman,[15] R. Willson,[20] S.W. Wissink,[12] R. Witt,[33] J. Wood,[6] N. Xu,[15] Z. Xu,[2] A. E. Yakutin,[22] E. Yamamoto,[15] J. Yang,[6] P. Yepes,[24] V. I. Yurevich,[9] Y.V. Zanevski,[9] I. Zborovský,[9] H. Zhang,[33] W. M. Zhang,[14] R. Zoulkarneev,[10] and A. N. Zubarev[9]

(STAR Collaboration)

[1]*Argonne National Laboratory, Argonne, Illinois 60439*
[2]*Brookhaven National Laboratory, Upton, New York 11973*
[3]*University of Birmingham, Birmingham, United Kingdom*
[4]*University of California, Berkeley, California 94720*
[5]*University of California, Davis, California 95616*
[6]*University of California, Los Angeles, California 90095*
[7]*Carnegie Mellon University, Pittsburgh, Pennsylvania 15213*
[8]*Creighton University, Omaha, Nebraska 68178*
[9]*Laboratory for High Energy (JINR), Dubna, Russia*

[10]Particle Physics Laboratory (JINR), Dubna, Russia
[11]University of Frankfurt, Frankfurt, Germany
[12]Indiana University, Bloomington, Indiana 47408
[13]Institut de Recherches Subatomiques, Strasbourg, France
[14]Kent State University, Kent, Ohio 44242
[15]Lawrence Berkeley National Laboratory, Berkeley, California 94720
[16]Max-Planck-Institut für Physik, Munich, Germany
[17]Michigan State University, East Lansing, Michigan 48824
[18]Moscow Engineering Physics Institute, Moscow, Russia
[19]City College of New York, New York City, New York 10031
[20]Ohio State University, Columbus, Ohio 43210
[21]Pennsylvania State University, University Park, Pennsylvania 16802
[22]Institute of High Energy Physics, Protvino, Russia
[23]Purdue University, West Lafayette, Indiana 47907
[24]Rice University, Houston, Texas 77251
[25]Universidade de Sao Paulo, Sao Paulo, Brazil
[26]SUBATECH, Nantes, France
[27]Texas A&M, College Station, Texas 77843
[28]University of Texas, Austin, Texas 78712
[29]Warsaw University of Technology, Warsaw, Poland
[30]University of Washington, Seattle, Washington 98195
[31]Wayne State University, Detroit, Michigan 48201
[32]Institute of Particle Physics, CCNU (HZNU), Wuhan 430079, China
[33]Yale University, New Haven, Connecticut 06520
(Received 7 June 2002; published 20 December 2002)

The STAR Collaboration reports the first observation of exclusive ρ^0 photoproduction, AuAu $\rightarrow$ AuAuρ^0, and ρ^0 production accompanied by mutual nuclear Coulomb excitation, AuAu $\rightarrow$ Au*Au$^\star\rho^0$, in ultraperipheral heavy-ion collisions. The ρ^0 have low transverse momenta, consistent with coherent coupling to both nuclei. The cross sections at $\sqrt{s_{NN}} = 130$ GeV agree with theoretical predictions treating ρ^0 production and Coulomb excitation as independent processes.

DOI: 10.1103/PhysRevLett.89.272302 PACS numbers: 25.75.Dw, 13.60.–r, 25.20.–x

In ultraperipheral heavy-ion collisions, the two nuclei geometrically "miss" each other and no hadronic nucleon-nucleon collisions occur. At impact parameters b significantly larger than twice the nuclear radius R_A, the nuclei interact by photon exchange and photon-photon or photon-Pomeron collisions [1]. Examples are nuclear Coulomb excitation, electron-positron pair and meson production, and vector meson production. The exchange bosons can couple coherently to the nuclei, yielding large cross sections. Coherence restricts the final states to low transverse momenta, a distinctive experimental signature. The STAR Collaboration reports the first observation of coherent exclusive ρ^0 photoproduction, AuAu $\rightarrow$ AuAuρ^0, and coherent ρ^0 production accompanied by mutual nuclear excitation, AuAu $\rightarrow$ Au*Au$^\star\rho^0$. Ultraperipheral heavy-ion collisions complement fixed-target ρ^0 photoproduction on complex nuclei [2].

Exclusive ρ^0 meson production, AuAu $\rightarrow$ AuAuρ^0 [c.f. Figure 1(a)], can be described by the Weizsäcker-Williams approach [3] to the photon flux and the vector meson dominance model [4]. A photon emitted by one nucleus fluctuates to a virtual ρ^0 meson, which scatters elastically from the other nucleus. The gold nuclei are not disrupted, and the final state consists solely of the two nuclei and the vector meson decay products [5]. In the rest frame of the target nucleus, midrapidity ρ^0 production at the Relativistic Heavy-Ion Collider (RHIC) corresponds to a photon energy of 50 GeV and a photon-nucleon center-of-mass energy of 10 GeV. In addition to coherent ρ^0 production, the exchange of virtual photons may excite the nuclei. These processes are assumed to factorize for heavy-ion collisions, which is justified by the similar case of two-photon interactions in relativistic ion collisions accompanied by nuclear breakup, where nonfactorizable diagrams are small [6]. The process AuAu $\rightarrow$ Au*Au$^\star\rho^0$ is shown in Fig. 1(b). In lowest order, mutual nuclear excitation of heavy ions occurs by the exchange of two photons [7,8]. Because of the Coulomb barrier for

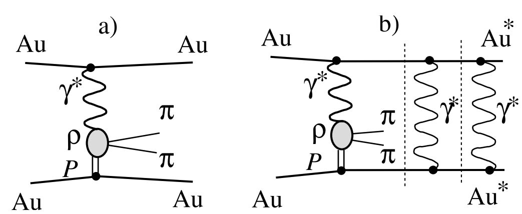

FIG. 1. Diagram for (a) exclusive ρ^0 production in ultraperipheral heavy-ion collisions, and (b) ρ^0 production with nuclear excitation. The dashed lines indicate factorization.

the emission of charged particles, nearly all nuclear decays following photon absorption include neutron emission [9].

The photon and Pomeron can couple coherently to the gold nuclei. The wavelength $\lambda_{\gamma,\mathcal{P}} > 2R_A$ leads to coherence conditions: a low transverse momentum of $p_T < \pi\hbar/R_A$ (~ 90 MeV/c for gold with $R_A \sim 7$ fm), and a maximum longitudinal momentum of $p_\parallel < \pi\hbar\gamma/R_A$ ($\sim$ 6 GeV/c at $\gamma = 70$), where γ is the Lorentz boost of the nucleus. The photon flux is proportional to the square of the nuclear charge Z^2 [3], and the forward cross section for elastic $\rho^0 A$ scattering $d\sigma^{\rho A}/dt|_{t=0}$ scales as $A^{4/3}$ for surface coupling and A^2 in the bulk limit. At a center-of-mass energy of $\sqrt{s_{NN}} = 130$ GeV per nucleon-nucleon pair, a total ρ^0 cross section, regardless of nuclear excitation, $\sigma(\mathrm{AuAu} \rightarrow \mathrm{Au}^{(\star)}\ \mathrm{Au}^{(\star)}\rho^0) = 350$ mb is predicted from a Glauber extrapolation of $\gamma p \rightarrow \rho^0 p$ data [5]. Calculations for coherent ρ^0 production with nuclear excitation assume that both processes are independent, sharing only a common impact parameter [5,7].

In the year 2000, the RHIC at Brookhaven National Laboratory collided gold nuclei at $\sqrt{s_{NN}} = 130$ GeV. In the Solenoidal Tracker at RHIC (STAR) [10], charged particles are reconstructed with a cylindrical time projection chamber (TPC) [11] operated in a 0.25 T solenoidal magnetic field. A central trigger barrel (CTB) of 240 scintillator slats surrounds the TPC. Two zero degree hadron calorimeters (ZDCs) at ± 18 m from the interaction point are sensitive to the neutral remnants of nuclear breakup, with $98 \pm 2\%$ acceptance for neutrons from nuclear breakup through Coulomb excitation [8,12].

Exclusive ρ^0 production has a distinctive signature: the $\pi^+\pi^-$ from the ρ^0 decay in an otherwise "empty" detector. The tracks are approximately back to back in the transverse plane due to the small p_T of the pair. The gold nuclei remain undetected within the beam.

Two data sets are used in this analysis. For $\mathrm{AuAu} \rightarrow \mathrm{AuAu}\rho^0$, about 30 000 events were collected using a low-multiplicity "topology" trigger. The CTB was divided in four azimuthal quadrants. Single hits were required in the opposite side quadrants; the top and bottom quadrants acted as vetoes to suppress cosmic rays. A fast on-line reconstruction [13] removed events without reconstructible tracks from the data stream. To study $\mathrm{AuAu} \rightarrow \mathrm{Au}^\star\mathrm{Au}^\star\rho^0$, a data set of about 800 000 "minimum bias" events, which required coincident detection of neutrons in both ZDCs as a trigger, is used.

Events are selected with exactly two oppositely charged tracks forming a common vertex within the interaction region. The ρ^0 candidates are accepted within a rapidity range $|y_\rho| < 1$. A systematic uncertainty of 5% is assigned to the number of ρ^0 candidates by varying the event selection criteria. The specific energy loss dE/dx in the TPC shows that the event sample is dominated by pion pairs. Without the ZDC requirement in the topology trigger, cosmic rays are a major background. They are removed by requiring that the two pion tracks have an opening angle of <3 rad. Using the energy deposits in the ZDCs, we select events with at least one neutron (xn, xn), exactly one neutron $(1n, 1n)$, or no neutrons $(0n, 0n)$ in each ZDC, and events with at least one neutron in exactly one ZDC $(xn, 0n)$; the latter two occur only in the topology trigger. A 10% uncertainty arises from the selection of single neutron signals.

The uncorrected transverse momentum spectra of pion pairs for the two-track event samples of the topology trigger $(0n, 0n)$ and the minimum bias trigger (xn, xn) are shown in Fig. 2. Both spectra are peaked at $p_T \sim 50$ MeV/c, as expected for coherent coupling. A background model from like-sign combination pairs, normalized to the signal at $p_T > 200$ MeV/c, is not peaked. For comparison, the p_T spectra from Monte Carlo simulations [5] discussed below are shown. They are normalized to the ρ^0 signal at $p_T < 150$ MeV/c and added to the background. The $M_{\pi\pi}$ invariant mass spectra (c.f. Figure 4) for both event samples are peaked around the ρ^0 mass. We find 131 ± 14 $(0n, 0n)$ and 656 ± 36 (xn, xn) events at $p_T < 150$ MeV/c, which we define as coherent ρ^0 candidates.

The data contain combinatorial background contributions from grazing nuclear collisions and incoherent photon-nucleon interactions, which are statistically subtracted. Incoherent ρ^0 production, where a photon interacts with a single nucleon, yields high p_T ρ^0, which are suppressed by the low pair p_T requirement; the remaining small contribution is indistinguishable from the coherent process. A coherently produced background arises from the misidentified two-photon process $\mathrm{AuAu} \rightarrow \mathrm{Au}^{(\star)}\mathrm{Au}^{(\star)}l^+l^-$. It contributes mainly at low invariant mass $M_{\pi\pi} < 0.5$ GeV/c^2. Electrons with momenta $p < 140$ MeV/c can be identified by their energy loss dE/dx. About 30 e^+e^- pairs, peaked at low pair $p_T \sim 20$ MeV/c, were detected in the minimum bias data sample [14]. They are extrapolated to the full phase space using a Monte Carlo simulation that describes e^+e^- pair

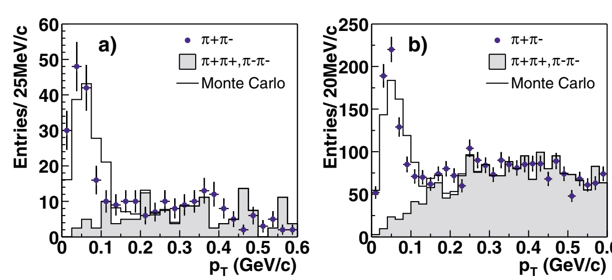

FIG. 2 (color online). The p_T spectra of pion pairs for the two-track events selected by (a) the topology trigger $(0n, 0n)$ and (b) the minimum bias trigger (xn, xn). Points are oppositely charged pairs, and the shaded histograms are the normalized like-sign combinatorial background. The open histograms are simulated ρ^0 superimposed onto the background.

production by lowest order perturbation theory [15]. Electron-positron pairs contribute 4% ± 1% to the signal at $p < 150$ MeV/c and $M_\rho \pm 0.3$ GeV/c. For a given M_{ll}, muons have lower momenta than the corresponding electrons and are less likely to be detected. Their <2% contribution to the coherent signal, as well as the contribution from ω decays are neglected.

The acceptance and reconstruction efficiency were studied using a Monte Carlo event generator that reproduces the expected kinematic and angular distributions for ρ^0 production with and without nuclear excitation [5,16], coupled with a full detector simulation. The ρ^0 decay angle distribution is consistent with s-channel helicity conservation. The ρ^0 production angles are not reconstructed since the AuAu scattering plane cannot be determined. The efficiencies are almost independent of p_T and the reconstructed invariant mass $M_{\pi\pi}$. For the minimum bias trigger, $42\% \pm 5\%$ of all ρ^0 within $|y_\rho| < 1$ are reconstructed. The topology trigger vetoes the top and bottom of the TPC, reducing the geometrical acceptance. Pions with $p_T < 100$ MeV/c do not reach the CTB, effectively excluding pairs with $M_{\pi\pi} <$ 500 MeV/c^2. Only $7\% \pm 1\%$ of all ρ^0 with $|y_\rho| < 1$ are reconstructed in the topology trigger. The p_T resolution is 9 MeV/c. The $M_{\pi\pi}$ and rapidity resolutions are 11 MeV/c^2 and 0.01.

The rapidity distribution for ρ^0 candidates (xn, xn) from the minimum bias data is shown in Fig. 3(a). It is well described by the reconstructed events from a simulation, which includes nuclear excitation [5]. The generated rapidity distribution is also shown. The acceptance is small for $|y_\rho| > 1$, so this region is excluded from the analysis. Cross sections are extrapolated from $|y_\rho| < 1$ to the full 4π acceptance by $\sigma^\rho_{4\pi}/\sigma^\rho_{|y_\rho|<1} = 1.9$ for ρ^0 production with nuclear breakup, and $\sigma^\rho_{4\pi}/\sigma^\rho_{|y_\rho|<1} = 2.7$ for ρ^0 production without nuclear breakup. A 15% uncertainty in the extrapolations is estimated by varying the Monte Carlo parameters. Event rapidity and photon energy are related by $y = \pm(1/2)\ln(2E_\gamma/M_\rho)$. After accounting for the ambiguity of photon emitter and scattering target, the average photon energy $\langle E_\gamma \rangle \sim$ 50 GeV is independent of rapidity.

The minimum bias data sample has an integrated luminosity of $L = 59\ \mathrm{mb}^{-1}$. The luminosity was measured by counting hadronic collisions [17]. We assume a total gold-gold hadronic cross section of 7.2 b [7]; its uncertainty dominates the 10% systematic uncertainty of L.

The differential cross section $d\sigma(\gamma\mathrm{Au} \to \rho\mathrm{Au})/dt \sim d\sigma(\gamma\mathrm{Au} \to \rho\mathrm{Au})/dp_T^2$ for the (xn, xn) events is shown in Fig. 3(b). Here, the combinatorial background is subtracted. The photon flux is determined integrating the photon spectrum of a relativistic nucleus over the impact parameter space [5]. In ultraperipheral collisions, $d\sigma/dt$ reflects not only the nuclear form factor, but also the photon p_T distribution and the interference of production amplitudes from both gold nuclei. The interference arises since both nuclei can be either the photon source or the scattering target [18]. A detailed study of this effect is beyond the scope of this paper. From a fit to $d\sigma^{\rho\mathrm{Au}}/dt \propto e^{-bt}$, we obtain a forward cross section $d\sigma^{\rho A}/dt|_{t=0} = 965 \pm 140 \pm 230\ \mathrm{mb/GeV}^2$ and an approximate gold radius of $R_{\mathrm{Au}} = \sqrt{4b} = 7.5 \pm 2$ fm, comparable to previous results [2].

The $d\sigma(\mathrm{AuAu} \to \mathrm{Au}^*\mathrm{Au}^*\rho)/dM_{\pi\pi}$ invariant mass spectrum for the (xn, xn) events with a pair $p_T <$ 150 MeV/c is shown in Fig. 4; the $(0n, 0n)$ events have a similar $d\sigma/dM_{\pi\pi}$ spectrum. Three different parametrizations are applied:

$$d\sigma/dM_{\pi\pi} = f_\rho \mathrm{BW}(M_{\pi\pi}) + f_I I(M_{\pi\pi}) + f_p, \quad (1)$$

$$d\sigma/dM_{\pi\pi} = \left| A \frac{\sqrt{M_{\pi\pi} M_\rho \Gamma_\rho}}{M^2_{\pi\pi} - M^2_\rho + i M_\rho \Gamma_\rho} + B \right|^2 + f_p, \quad (2)$$

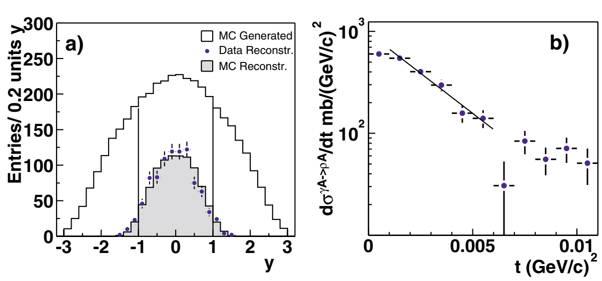

FIG. 3 (color online). Rapidity distribution (a) of ρ^0 candidates (xn, xn) for the minimum bias data (points) compared to the normalized reconstructed (shaded histogram) and generated (open histogram) events from the Monte Carlo simulation. The differential cross section (b) $d\sigma(\gamma Au \to \rho Au)/dt$ for the same data set; the line indicates the exponential fit.

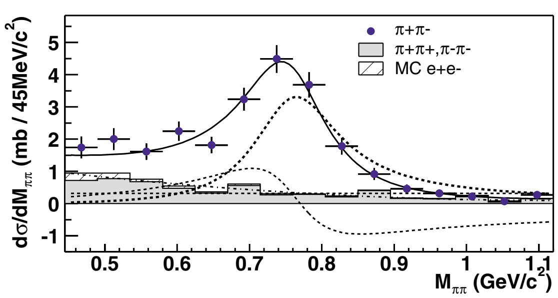

FIG. 4 (color online). The $d\sigma(\mathrm{AuAu} \to \mathrm{Au}^*\mathrm{Au}^*\rho)/dM_{\pi\pi}$ spectrum for two-track (xn, xn) events with pair-$p_T <$ 150 MeV/c in the minimum bias data. The shaded histogram is the combinatorial background, and the hatched histogram contains an additional contribution from coherent e^+e^- pairs. The fits correspond to Eq. (2): the sum (solid) of a Breit-Wigner, a mass-independent contribution from direct $\pi^+\pi^-$ production and their interference (dashed line), and a second order polynomial for the residual background (dash-dotted line).

TABLE I. Parameters for different mass fits.

Eq.	M_ρ (MeV/c^2)	Γ^0_ρ (MeV/c^2)	
1	778 ± 7	148 ± 14	$f_I/f_\rho = 0.47 \pm 0.07 \pm 0.12$ GeV
2	777 ± 7	139 ± 13	$\lvert B/A \rvert = 0.81 \pm 0.08 \pm 0.20$ GeV$^{-1/2}$
3	773 ± 7	127 ± 13	$n = 5.7 \pm 0.4 \pm 1.5$

$$d\sigma/dM_{\pi\pi} = f_\rho \mathrm{BW}(M_{\pi\pi})(m_\rho/M_{\pi\pi})^n + f_p. \quad (3)$$

Equation (1) is a relativistic Breit-Wigner, $\mathrm{BW} = M_{\pi\pi}M_\rho\Gamma_\rho/[(M_\rho^2 - M_{\pi\pi}^2)^2 + M_\rho^2\Gamma_\rho^2]$, for ρ^0 production plus a Söding interference term [19], $I(M_{\pi\pi}) = (M_\rho^2 - M_{\pi\pi}^2)/[(M_\rho^2 - M_{\pi\pi}^2)^2 + M_\rho^2\Gamma_\rho^2]$, Eq. (2) is a modified Söding parametrization [20], and Eq. (3) is a phenomenological Ross-Stodolsky parametrization [21]. Here, $\Gamma_\rho = \Gamma_0 \cdot (M_\rho/M_{\pi\pi}) \cdot [(M_{\pi\pi}^2 - 4m_\pi^2)/(M_\rho^2 - 4m_\pi^2)]^{3/2}$ is the momentum-dependent width, and f_p is a fixed second order polynomial describing the residual background. The fit parameters are given in Table I. The ρ^0 mass and width are consistent with accepted values [22]; they were fixed to reduce the number of degrees of freedom to obtain $|B/A|$, f_I/f_ρ, and n. Our results are consistent with values found for the same parametrizations in $\gamma p \to \rho^0 p$ photoproduction data [20,23].

For coherent ρ^0 production accompanied by mutual nuclear breakup (xn, xn), we measure a cross section of $\sigma(\mathrm{AuAu} \to \mathrm{Au}^*_{xn}\mathrm{Au}^*_{xn}\rho^0) = 28.3 \pm 20.0 \pm 6.3$ mb in the two-track event sample, by extrapolating the integral of the Breit-Wigner fit to full rapidity. By selecting single neutron signals in both ZDCs, we obtain $\sigma^\rho_{1n,1n}/\sigma^\rho_{xn,xn} = 0.097 \pm 0.014$, so $\sigma(\mathrm{AuAu} \to \mathrm{Au}^*_{1n}\mathrm{Au}^*_{1n}\rho^0) = 2.8 \pm 0.5 \pm 0.7$ mb. Single neutron emission is predominantly due to Coulomb excitation and the subsequent decay of the giant dipole resonance. The ratio $\sigma^\rho_{1n,1n}/\sigma^\rho_{xn,xn}$ is consistent with $\sigma_{1n,1n}/\sigma_{xn,xn} = 0.12 \pm 0.01$ found for mutual Coulomb dissociation at RHIC [8], supporting that ρ^0 production and nuclear excitation are independent processes.

At $b \sim 2R_A$, coherent ρ^0 photoproduction can overlap with grazing nuclear collisions, producing a low $p_T\rho^0$ accompanied by additional tracks. Additional tracks can also be produced at $b > 2R_A$ from nuclear excitation by high energy photons. At present, we cannot differentiate between these two processes. The coherent (xn, xn) ρ^0 sample increases by 40% when events with additional tracks are included. Accounting for this, we find $\sigma^{(\mathrm{inc.\ overlap})}(\mathrm{AuAu} \to \mathrm{Au}^*_{xn}\mathrm{Au}^*_{xn}\rho^0) = 39.7 \pm 2.8 \pm 9.7$ mb. For $(1n, 1n)$ events, no additional ρ^0 candidates are found with higher track multiplicities.

The major systematic uncertainties are in the 4π extrapolation (15%), acceptance and reconstruction efficiency (12%), luminosity determination (10%), and event selection (5%). The overlap region with grazing nuclear collisions contributes 10%; it does not contribute to $\sigma^\rho_{1n,1n}$, but a 10% uncertainty is due to the selection of the single neutrons. These contributions add in quadrature to 24% systematic uncertainty in the cross sections.

The absolute efficiency of the year 2000 topology trigger is poorly known and does not allow a direct cross section measurement. From the two-track events, we obtain the cross section ratios $\sigma^\rho_{xn,xn}/\sigma^\rho_{0n,0n} = 0.09 \pm 0.04$ and $\sigma^\rho_{xn,xn}/\sigma^\rho_{xn,0n} = 0.30 \pm 0.19$. The uncertainties reflect the small number of (xn, xn) and $(xn, 0n)$ events in the topology trigger data. Grazing nuclear collisions do not contribute to $\sigma^\rho_{0n,0n}$ and $\sigma^\rho_{xn,0n}$, since they yield neutron signals in both ZDCs. From $\sigma(\mathrm{AuAu} \to \mathrm{Au}^*_{xn}\mathrm{Au}^*_{xn}\rho^0)$, we estimate $\sigma(\mathrm{AuAu} \to \mathrm{AuAu}\rho^0) = 370 \pm 170 \pm 80$ mb, $\sigma(\mathrm{AuAu} \to \mathrm{Au}^*_{xn}\mathrm{Au}\rho^0) = 95 \pm 60 \pm 25$ mb, and the total cross section for coherent ρ^0 production $\sigma(\mathrm{AuAu} \to \mathrm{Au}^{(*)}\mathrm{Au}^{(*)}\rho^0) = 460 \pm 220 \pm 110$ mb. Table II compares our results to the calculations of Ref. [5]. The calculation for $\sigma^\rho_{xn,xn}$ excludes grazing nuclear collisions; it is therefore compared to our value without the overlap correction. Recent predictions [24] are about 50% higher than in Ref. [5] without giving specific numbers for $\sqrt{s_{NN}} = 130$ GeV.

In summary, the first measurements of coherent ρ^0 production with and without accompanying nuclear excitation, $\mathrm{AuAu} \to \mathrm{Au}^\star\mathrm{Au}^\star\rho^0$ and $\mathrm{AuAu} \to \mathrm{AuAu}\rho^0$, confirm the existence of vector meson production in ultra-peripheral heavy-ion collisions. The ρ^0 are produced at small transverse momentum, showing the coherent coupling to both nuclei. The cross sections at $\sqrt{s_{NN}} = 130$ GeV are in agreement with theoretical calculations.

We thank the RHIC Operations Group and the RHIC Computing Facility at Brookhaven National Laboratory, and the National Energy Research Scientific Computing Center at Lawrence Berkeley National Laboratory for their support. This work was supported by the Division of Nuclear Physics and the Division of High Energy

TABLE II. Comparison to predictions from [5]. The uncertainties are highly correlated.

Cross section	STAR (mb)	Ref. [5] (mb)
$\sigma^\rho_{xn,xn}$	28.3 ± 2.0 ± 6.3	27
$\sigma^\rho_{1n,1n}$	2.8 ± 0.5 ± 0.7	2.6
$\sigma^{\rho(\mathrm{inc.\ overlap})}_{xn,xn}$	39.7 ± 2.8 ± 9.7	⋯
$\sigma^\rho_{xn,0n}$	95 ± 60 ± 25	⋯
$\sigma^\rho_{0n,0n}$	370 ± 170 ± 80	⋯
$\sigma^\rho_{\mathrm{total}}$	460 ± 220 ± 110	350

Physics of the Office of Science of the U.S. Department of Energy, the United States National Science Foundation, the Bundesministerium für Bildung und Forschung of Germany, the Institut National de la Physique Nucleaire et de la Physique des Particules of France, the United Kingdom Engineering and Physical Sciences Research Council, Fundacao de Amparo a Pesquisa do Estado de Sao Paulo, Brazil, the Russian Ministry of Science and Technology and the Ministry of Education of China, and the National Natural Science Foundation of China.

[1] G. Baur, K. Hencken, and D. Trautmann, J. Phys. G **24**, 1657 (1998); G. Baur *et al.*, Phys. Rep. **364**, 359 (2002).
[2] F. Bulos *et al.*, Phys. Rev. Lett. **22**, 490 (1969); H. Alvensleben *et al.*, Phys. Rev. Lett. **24**, 786 (1970); **24** 792 (1970); Nucl. Phys. **B18**, 333 (1970); G. McClellan *et al.*, Phys. Rev. D **4**, 2683 (1971).
[3] C. F. v. Weizsäcker, Z. Phys. **88**, 612 (1934); E. J. Williams, Phys. Rev. **45**, 729 (1934).
[4] J. J. Sakurai, Ann. Phys. (Leipzig) **11**, 1 (1960); T. H. Bauer *et al.*, Rev. Mod. Phys. **50**, 261 (1978).
[5] S. R. Klein and J. Nystrand, Phys. Rev. C **60**, 014903 (1999); A. J. Baltz, S. R. Klein, and J. Nystrand, Phys. Rev. Lett. **89**, 012301 (2002). The cross sections for $\sqrt{s_{NN}} = 130$ GeV are a private communication.
[6] K. Hencken, D. Trautmann, and G. Baur, Z. Phys. C **68**, 473 (1995).
[7] A. J. Baltz, C. Chasman, and S. N. White, Nucl. Instrum. Methods Phys. Res., Sect. A **417**, 1 (1998).
[8] M. Chiu *et al.*, Phys. Rev. Lett. **89**, 012302 (2002).
[9] B. L. Berman and S. C. Fultz, Rev. Mod. Phys. **47**, 713 (1975).
[10] K. H. Ackermann *et al.*, Nucl. Phys. **A661**, 681c (1999).
[11] H. Wieman *et al.*, IEEE Trans. Nucl. Sci. **44**, 671 (1997).
[12] C. Adler *et al.*, Nucl. Instrum. Methods Phys. Res., Sect. A **470**, 488 (2001).
[13] J. S. Lange *et al.*, Nucl. Instrum. Methods Phys. Res., Sect. A **453**, 397 (2000).
[14] F. Meissner, nucl-ex/0112008.
[15] S. R. Klein and E. Scannapieco, STAR Note 243 (1996).
[16] J. Nystrand and S. R. Klein, nucl-ex/9811007.
[17] C. Adler *et al.*, Phys. Rev. Lett. **87**, 112303 (2001).
[18] S. R. Klein and J. Nystrand, Phys. Rev. Lett. **84**, 2330 (2000).
[19] P. Söding, Phys. Lett. **19**, 702 (1966).
[20] J. Breitweg *et al.*, Eur. Phys. J. C **2**, 247 (1998).
[21] M. Ross and L. Stodolsky, Phys. Rev. **149**, 1172 (1966).
[22] D. E. Groom *et al.*, Eur. Phys. J. C **15**, 1 (2000).
[23] S. Aid *et al.*, Nucl. Phys. **B463**, 3 (1996).
[24] L. Frankfurt, M. Strikman, and M. Zhalov, Phys. Lett. B **537**, 51 (2002).